

Thermal Properties of High-Volume Fly Ash Mortars and Concretes

D.P. Bentz*

M.A. Peltz

Building and Fire Research Laboratory
National Institute of Standards and Technology
100 Bureau Drive, Stop 8615
Gaithersburg, MD 20899-8615 USA

A. Durán-Herrera

P. Valdez

C. Juárez

Academic Group on Concrete Technology
Universidad Autónoma de Nuevo León
Monterrey, Nuevo León, MEXICO

* D.P. Bentz: dale.bentz@nist.gov, Phone: (301)975-5865, FAX: (301)990-6891

Abstract

As sustainability moves to the forefront of construction, the utilization of high volume fly ash concrete mixtures to reduce CO₂ emissions and cement consumption per unit volume of concrete placed is receiving renewed interest. Concrete mixtures in which the fly ash replaces 50 % or more of the portland cement are both economically and technically viable. This paper focuses on a characterization of the thermal properties, namely heat capacity and thermal conductivity, of such mixtures. Both the raw materials and the finished products (mortars and concretes) are evaluated using a transient plane source method. Because the specimens being examined are well hydrated, estimates of the heat capacity based on a law of mixtures with a “bound water” heat capacity value employed for the water in the mixture provide reasonable predictions of the measured performance. As with most materials, thermal conductivity is found to be a function of density, while also being dependent on whether the aggregate source is siliceous or limestone. The measured values should provide a useful database for evaluating the thermal performance of high volume fly ash concrete structures.

Keywords: Building technology, density, heat capacity, high volume fly ash, sustainability, thermal conductivity.

Introduction

As part of a sustainability movement within the concrete industry, the increased utilization of high volume fly ash (HVFA) mixtures is being promoted (Mehta 2009). Typically in these mixtures, fly ash can replace 50 % or more of the portland cement, reducing cement consumption and the CO₂ emissions accompanying its production, on a per volume unit of concrete basis. While fresh concrete properties and mechanical properties of the hardened concrete have been investigated in detail for these mixtures (Bouzoubaa et al., 2001, Durán-Herrera et al., 2009, McCarthy and Dhir, 2005, Mehta, 2004), few studies of thermal properties have been performed. From a sustainability perspective, thermal properties such as heat capacity and thermal conductivity are critical in assessing the potential energy efficiency of HVFA concrete structures, such as residential and commercial buildings. For example, since the density of fly ash can be as much as 1/3rd less than that of cement (Bentz, 2009), HVFA concretes may exhibit a reduced thermal conductivity, making them more insulative than conventional concretes.

Dermiboga et al. (Dermiboga et al., 2007, Dermiboga, 2003a, Dermiboga, 2003b, Dermiboga and Gul, 2003) have reported extensively on the thermal properties of mixtures containing high volumes of mineral admixtures, but only for specimens that have been first extensively dried (to constant mass) at 110 °C, dramatically reducing their thermal conductivity for example. The goal of the present study is to provide heat capacity and thermal conductivity values for HVFA mortars and concretes that have been equilibrated under laboratory environmental conditions that are more representative of field exposures.

Experimental

The thermal properties of two sets of HVFA specimens were evaluated. The first set was from a series of HVFA mortars prepared by Bentz et al. (2010), for a study that examined the influence of cement type, fly ash type, and internal curing on performance. These mortars contained 50 % fly ash by mass replacement for cement (except for the control mixture without fly ash), a water-to-cementitious materials ratio (w/cm) of 0.3, and 54 % (siliceous) sand by volume fraction. Mixtures were prepared using either a Type I/II or a Type III cement (ASTM, 2009), either a class C or a class F fly ash (ASTM, 2009), and with or without internal curing, as supplied by pre-wetted lightweight aggregate sand replacing a portion of the silica sand. For the class C fly ash used with either cement, a 2 % addition of gypsum (calcium sulfate dihydrate) was necessary to achieve normal hydration characteristics, as determined by isothermal calorimetry measurements (Bentz, 2009). Thermal measurements were performed on 50.8 mm mortar cubes first cured for 182 d. Cubes without internal curing were cured in a lime-saturated solution, while those with internal curing were cured under sealed conditions in double plastic bags, both in a walk-in environmental chamber maintained at $25\text{ }^{\circ}\text{C} \pm 1\text{ }^{\circ}\text{C}$. Two cubes from each series were evaluated using the transient plane source (TPS) method to be described subsequently. Additionally, the heat capacities of the individual powders (cement, fly ash, and gypsum) and sands (normal weight and lightweight) were also measured using a gold pan heat capacity cell connected to the TPS measurement system.

The second set of specimens was based on a series of three concretes prepared in Mexico (Durán-Herrera et al., 2009) and shipped to the National Institute of Standards and Technology (NIST), with the mixture proportions as shown in Table 1. Mixtures were prepared using an ASTM C 595 Type IP (MS) cement (ASTM, 2009), and included three different w/cm (0.5, 0.55,

and 0.6) and fly ash contents by mass of 0 %, 15 %, 30 %, 45 %, 60 %, and 75 %, for eighteen mixtures in total. The fresh concrete and hardened concrete mechanical properties are summarized in Durán-Herrera et al. (2009), and the 28-d compressive strengths measured in that study are included in Table 1. For thermal measurements, specimens were prepared as a set of two 101.6 mm cubes per concrete mixture in Table 1, and were cured for 28 d prior to being shipped to the U.S. At NIST, the specimens were stored under laboratory conditions (nominally 23 °C and 40 % relative humidity (RH)) for between 28 d and 84 d, until being measured using the TPS method. The density of each cube was determined just prior to the thermal measurements, by measuring its mass and external dimensions. As shown in Figure 1, the measured densities were consistently slightly less than the unit weights of the corresponding fresh concrete, likely indicating some drying of the specimens during aging. The heat capacities of the cement and fly ash powders and the limestone sand were also determined on samples obtained directly from Mexico. It was assumed that the heat capacity of the coarse limestone aggregate would be the same as that measured for the limestone sand.

The TPS measurement technique has been described in detail by Gustafsson (1991) and Log and Gustafsson (1995), with theoretical considerations having been summarized by He (2005). For the current study, a 6.403 mm radius probe (Ni foil encased in Kapton) was selected. The probe was sandwiched horizontally between the cast sides of the twin hardened mortar cubes or the cut faces of two halves of a concrete cube. After an equilibration time of at least 45 min in a laboratory nominally maintained at 23 °C, measurements were obtained with a power of 0.3 W applied for a measurement time of 10 s. The measured response of the probe/sensor was analyzed using the built-in software to determine the thermal conductivity and volumetric heat capacity of the specimens. The volumetric heat capacity was then converted to a

mass basis by dividing by the measured average density of the twin specimens. The analyzer samples 200 points during the 10 s measurement time and typically points 75 to 200 were used in the quantitative analysis. For the mortar cubes, four or more individual cast faces were analyzed in this fashion, with the average value being reported. For the cut concrete cubes, eight areas (two for each side edge) were measured and the average value reported, after discarding obvious outliers as discussed below. According to the manufacturer's specifications, thermal conductivity measurements made in this way are reproducible within $\pm 2\%$ and heat capacity values with $\pm 7\%$.

For the separate heat capacity experiments on the powders and sands, approximately 0.4 g to 1.0 g of the material was placed in the heat capacity unit, consisting of a special probe attached to the base of a gold pan/lid. For these measurements, the gold pan with its lid is surrounded on all sides by polystyrene insulation, in an attempt to minimize energy loss. First, a reference measurement is made with an empty pan, followed by the measurement with the specimen placed in the pan. In this case, a power of 0.1 W was applied for a measurement time of 80 s and points 100 to 200 (of the total 200 sampled in the 80 s) were used in the quantitative analysis. Knowing the mass of the specimen, its heat capacity in units of J/(g•K) can be easily determined. According to the manufacturer, heat capacity measurements made in this way are reproducible within $\pm 2\%$.

Measuring the thermal properties of the concrete cubes proved to be more challenging than expected. Originally, it was planned to measure these properties using a pair of cubes and measuring on the cast surfaces, as was done successfully for the mortar cubes. However, due to the larger aggregate size and perhaps the higher w/cm in the concrete, etc., there was a significant edge effect, with the microstructure and density of the (mortar rich) surface layer being quite

different from the bulk of the concrete. This resulted in computed thermal conductivities being higher and heat capacities being lower than expected. In fact, the measured heat capacity values on a mass basis that were computed using the bulk densities of the concretes were typically well below the values of any of the individual raw materials, an impossibility according to the accepted law of mixtures for the heat capacity of composite materials (Bentz, 2007, Choktaweekarn et al., 2009). Thus, in an effort to obtain a more representative surface for performing the thermal property measurements, one of the cubes for each concrete mixture was sawn in half and the two sawn surfaces were used for subsequent TPS measurements. As will be demonstrated in the results section, these sawn surfaces produced thermal property values within the expected range for these materials. Still, occasionally from one up to three of the eight measurements performed for a given cube were discarded due to producing heat capacity values below the possible minimum value, perhaps due to placing the probe directly over a cut large coarse aggregate for example. On the average, discarding these values resulted in an absolute change in the computed thermal conductivity of $0.06 \text{ W}/(\text{m}\cdot\text{K})$ and in the computed mass-based heat capacity of $0.07 \text{ J}/(\text{g}\cdot\text{K})$.

Results and Discussion

The measured heat capacities for the raw materials for the mortars and concretes are provided in Tables 2 and 3, respectively. The measured values for the three cements are in good agreement with the value of $0.75 \text{ J}/(\text{g}\cdot\text{K})$ determined in a previous study (Bentz, 2007). For a fly ash with a specific gravity of 2.03, Krishnaiah and Singh (2006) determined values of $0.72 \text{ J}/(\text{g}\cdot\text{K})$, $0.73 \text{ J}/(\text{g}\cdot\text{K})$, and $0.73 \text{ J}/(\text{g}\cdot\text{K})$ at three different compaction levels, using a thermal probe technique; these values are in excellent agreement with those determined for the three fly ashes examined in the present study. Since the heat capacities of the powders and sands are

quite similar, with the exception of the gypsum added to the mortars containing a class C fly ash, changes in mixture proportions will impact heat capacity most prominently through any changes in water content, as the heat capacity of water is much larger than that of any other concrete ingredient, being 4.18 J/(g·K) at 23 °C. As the water becomes incorporated into hydration products and physically bound in the gel products, its effective heat capacity is significantly reduced. Waller et al. (1996) suggest using a value of 2.2 J/(g·K) for such bound water in concrete.

The law of mixtures shown in equation (1) has been applied previously to predict the heat capacity of both hydrating cement pastes (Bentz, 2007) and fly ash concretes (Choktaweekarn et al., 2009).

$$c_{conc}^p = c_{water}^p m_{water} + c_{cem}^p m_{cem} + c_{FA}^p m_{FA} + c_{sand}^p m_{sand} + c_{Cagg}^p m_{Cagg} \quad (1)$$

where c^p refers to heat capacity, m to mass fraction, and the subscripts *conc*, *water*, *cem*, *FA*, *sand*, and *Cagg* correspond to concrete, water, cement, fly ash, sand, and coarse aggregate, respectively. As mentioned above, the complication in applying this equation is in knowing what value to use for the heat capacity of water. For a given mixture design, upper and lower bounds on the heat capacity may be computed by using the free water value of 4.18 J/(g·K) and the bound water estimate of 2.2 J/(g·K), respectively.

The measured heat capacities for the HVFA mortars and concretes are provided in Figures 2 and 3, respectively. In Figure 2, the values are plotted against the measured average density of the mortar cubes, while in Figure 3, they are plotted against the mass fraction of fly ash in the cementitious binder of the concrete. The mortar specimens were prepared with a low w/cm of 0.3 and cured for 182 d, so that the majority of the water should be bound as opposed to free capillary water. In agreement with this, using equation (1) with the bound water value of

heat capacity for water provides estimates ranging between 0.85 J/(g·K) and 0.91 J/(g·K) for the various mortars. In general, the experimental values in Figure 2 are slightly larger than this, as those mortars without internal curing were stored in lime-saturated water during the 182 d and have thus imbibed some of the curing solution, concurrently increasing their heat capacity above the bound water-based estimate. For the nine mortar mixtures measured in this study, the average heat capacity was 0.93 J/(g·K), with a standard deviation of 0.06 J/(g·K). This value compares favorably to the typical specific heats of concrete provided by Tatro (2006) that range from 0.917 J/(g·K) at 10 °C to 1.038 J/(g·K) at 66 °C.

Since the concretes were cured for an extended period under laboratory conditions of nominally 23 °C and 40 % RH prior to the thermal measurements, they did not have an opportunity to imbibe curing solution, undergoing drying instead. Thus, as shown in Figure 3, their measured heat capacities lie even closer to the average bound water estimate based on equation (1), using their initial mixture proportions given in Table 1. For the eighteen concrete mixtures measured in this study, the average heat capacity was 0.88 J/(g·K), with a standard deviation of 0.08 J/(g·K). Once again, the values measured for these concretes are near that given by Tatro (2006) for a typical concrete at 10 °C. In Figure 3, it can be observed that the mass fraction of fly ash has little influence on the measured heat capacity, since the heat capacities of the fly ash and cement are quite similar (Table 3). One might expect a higher w/cm concrete to exhibit a higher heat capacity, but a careful examination of Table 1 reveals that the actual water contents of the $w/cm=0.55$ and $w/cm=0.60$ concretes were identical, while that of the $w/cm=0.5$ concretes was only 5 % lower. Thus, within the uncertainty of the heat capacity measurements, no discernible trends between heat capacity and w/cm are observed in Figure 3.

Figure 4 summarizes the measured thermal conductivities for both HVFA mortar and concrete specimens. Because the thermal conductivity of siliceous aggregates is generally greater than that of limestone (Horai, 1971, Bougerra et al., 1997, Kim et al., 2003), the values measured for the mortars prepared with siliceous sand are higher than those for the concretes of an equivalent density, prepared with limestone sand and limestone coarse aggregates. For the limited density ranges examined for each system in this study, a linear function provides an adequate fit to the measured data. Other studies covering a wider range of lower densities have employed a power-law function with density as the exponent to fit the thermal conductivity vs. density data (Blanco et al., 2000). A power-law relationship is also clearly indicated for the concrete data contained in the NIST Standard Reference Database 81 - NIST Heat Transmission Properties of Insulating and Building Materials (Zarr, 2000), with the majority of that data being for lightweight concrete and concrete block (densities below 2000 kg/m^3).

For both the HVFA mortars and concretes, the results in Figure 4 indicate that significant reductions in thermal conductivity are possible by incorporating high volumes of fly ash into concrete. In the case of the mortars, the greatest reduction in thermal conductivity (45 %) was achieved by modifying the control (no fly ash) mixture to produce a mixture with 50 % fly ash and internal curing supplied by lightweight aggregates (further reducing the thermal conductivity due to their low density). For the mixtures without internal curing, replacing 50 % of the cement with fly ash produced reductions in thermal conductivity of 15 % and 7 % for class C and class F fly ashes, respectively. For the $w/cm=0.5$ concretes, the system with 75 % replacement of cement by fly ash exhibited a thermal conductivity that was 19 % lower than the control concrete prepared with 100 % IP (MS) blended cement. Reducing the thermal conductivity will increase

the insulation value provided by the concrete, reducing heating and cooling costs for residential and commercial buildings constructed of HVFA concrete.

The results in Figure 4 clearly indicate that both density and aggregate type have a strong influence on thermal conductivity. For applications where a low k is desired, limestone aggregates may be a superior choice relative to their siliceous counterparts, although it may be necessary to also account for the variability in k with aggregate quarry source for a given mineral type (Horai, 1971, Kim et al., 2003). For applications where further reductions in thermal conductivity are desirable, sustainable options would include the utilization of cenospheres (from coal-burning power plants) to produce lightweight concrete (Blanco et al., 2000) or the use of cold-bonded fly ash aggregates (Joseph and Ramamurthy, 2009).

For mass concrete applications, thermal performance is also characterized in terms of thermal diffusivity. Concrete with a high thermal diffusivity will rapidly adjust its temperature to match that of its surroundings. Therefore, often a low thermal diffusivity is preferred so that the concrete may act as a heat sink/source to buffer temperature extremes experienced during a diurnal cycle. Thermal diffusivity is defined as the ratio of thermal conductivity to volumetric heat capacity:

$$\alpha = \frac{k}{\rho c_p} \quad (2)$$

where α is thermal diffusivity, k thermal conductivity, ρ density, and c_p heat capacity on a mass basis. Since the heat capacity variation amongst the mortars and concretes is minimal, one can qualitatively examine their thermal diffusivities based on the densities and thermal conductivities provided in the single graph in Figure 4. While a reduced thermal conductivity will reduce thermal diffusivity, this may be offset by the reduction in density necessary to achieve the lower k . For the HVFA mortars examined in this study, the proportional change in thermal

conductivity is greater than that in density, so that the thermal diffusivity is decreased with increasing fly ash content as shown in Figure 5. Thus, the HVFA mortar with internal curing that produced a 45 % reduction in k , also produced a 36 % reduction in α . Conversely, for the HVFA concretes, the slope of the k vs. density data in Figure 4 is much less, so that the thermal diffusivities are nominally the same in Figure 5, with an average value of $9.9 \times 10^{-7} \text{ m}^2/\text{s}$ and a standard deviation of $0.7 \times 10^{-7} \text{ m}^2/\text{s}$. This suggests that for HVFA concretes prepared with limestone aggregates, a single value of thermal diffusivity may be appropriate for design purposes. This value is about 1/3rd less than the value of $1.53 \times 10^{-6} \text{ m}^2/\text{s}$ presented by Tatrow (2006), as a typical thermal diffusivity for limestone-based concrete.

Conclusions

The transient plane method can be employed to measure the thermal properties of high volume fly ash mortars and concretes at room temperature, providing values for both heat capacity and thermal conductivity. The measured heat capacity values for the well-aged specimens examined in the current study can be adequately predicted using a simple law of mixtures with a bound water estimate of 2.2 J/(g·K) for the water in the initial mixture proportions. Because the heat capacities of fly ashes and cements are quite similar, little difference in heat capacity is produced by replacing cement with fly ash. Conversely, due to its significantly reduced density, the addition of fly ash can substantially reduce the thermal conductivity of a mortar or concrete. The study has also highlighted the significant influence of aggregate type (siliceous vs. limestone) on thermal conductivity. By reducing thermal conductivity, HVFA mixtures may reduce heating and cooling costs for residential and commercial concrete buildings.

Acknowledgements

The provision of materials by BASF Mexicana S.A. de C.V., Cementos Moctezuma S.A. de C.V., the Federal Commission of Electricity of México, Industrializadora de Caliza S.A. de C.V., Lehigh Cement Corporation, Northeast Solite Corporation, the National Ready-Mixed Concrete Association, Separation Technologies, Inc., U.S. Concrete, and W.R. Grace & Co. – Conn. is gratefully acknowledged.

References

ASTM International, 2009. Annual Book of ASTM Standards, Vol. 04.01. Cement, Lime, and Gypsum, ASTM International, West Conshohocken, PA.

Bentz, D.P., 2007. Transient Plane Source Measurements of the Thermal Properties of Hydrating Cement Pastes. *Materials and Structures* 40, 1073-1080.

Bentz, D.P., 2009. Powder Additions to Mitigate Retardation in High Volume Fly Ash Mixtures. *ACI Materials Journal*, submitted.

Bentz, D.P., Ferraris, C.F., Peltz, M.A., Winpiger, J. 2010. Mixture Proportioning Options for Improving High Volume Fly Ash Concretes. In *Proceedings of the International Conference on Sustainable Concrete Pavements: Practices, Challenges, and Directions*, Sacramento, CA.

Blanco, F., Garcia, P., Mateos, P., Ayala, J. 2000. Characteristics and Properties of Lightweight Concrete Manufactured with Cenospheres. *Cement and Concrete Research* 30, 1715-1722.

Bouguerra, A., Laurent, J.P., Goual, M.S., Queneudec, M., 1997. The Measurement of the Thermal Conductivity of Solid Aggregates Using the Transient Plane Source Technique. *Journal of Physics D: Applied Physics* 30, 2900-2904.

Bouzoubaa, N., Zhang, M.-H., Malhotra, V.M. 2001. Mechanical Properties and Durability of Concrete Made with High-Volume Fly Ash Blended Cements using a Coarse Fly Ash. *Cement and Concrete Research* 31, 1393-1402.

Choktaweekarn, P., Saengsoy, W., Tangfermsirikul, S., 2009. A Model for Predicting the Specific Heat Capacity of Fly-Ash Concrete. *ScienceAsia* 35, 1788-182.

Demirboga, R., Turkmen, I., Karakoc, M.B., 2007. Thermo-mechanical Properties of Concrete Containing High-Volume Mineral Admixtures. *Building and Environment* 42, 349-354.

Demirboga, R., 2003a. Thermo-mechanical Properties of Sand and High Volume Mineral Admixtures. *Energy and Buildings* 35, 435-439.

Demirboga, R., 2003b. Influence of Mineral Admixtures on Thermal Conductivity and Compressive Strength of Mortar. *Energy and Buildings* 35, 189-192.

Demirboga, R., Gul, R., 2003. The Effects of Expanded Perlite Aggregate, Silica Fume, and Fly Ash on the Thermal Conductivity of Lightweight Concrete. *Cement and Concrete Research* 33, 723-727.

Durán-Herrera, A., Valdez, P., Rivera-Torres, J., 2009. Synergetic Effect of a Polycarboxylate Superplasticizer and a Fly Ash in the Production of a Concrete with Conventional Water/Binder Ratios. *Proceedings of the ACI/CANMET conference: Superplasticizers and Other Chemical Admixtures in Concrete – Recent Advances in Concrete Technology and Sustainability Issues*, Sevilla, Spain.

Gustafsson, S.E., 1991. Transient Plane Source Techniques for Thermal Conductivity and Thermal Diffusivity Measurements of Solid Materials. *Review of Scientific Instruments* 62, 797-804.

He, Y., 2005. Rapid Thermal Conductivity Measurement with a Hot Disk Sensor Part 1. Theoretical Considerations. *Thermochimica Acta* 436, 122-129.

Horai, K., 1971. Thermal Conductivity of Rock-Forming Minerals. *Journal of Geophysical Research* 76, 1278-1308.

Joseph, G., Ramamurthy, K., 2009. Autogenous Curing of Cold-Bonded Fly Ash Aggregate Concrete. Submitted to *ASCE Journal of Materials in Civil Engineering*.

Kim, K.-H., Jeon, S.-E., Kim, J.-K., Yang, S., 2003. An Experimental Study on Thermal Conductivity of Concrete. *Cement and Concrete Research* 33, 363-371.

Krishnaiah, S., Singh, D.N., 2006. Determination of Thermal Properties of Some Supplementary Cementing Materials Used in Cement and Concrete. *Construction and Building Materials* 20, 193-198.

Log, T. and Gustafsson, S.E., 1995. Transient Plane Source (TPS) Technique for Measuring Thermal Transport Properties of Building Materials. *Fire and Materials* 19, 43-49.

McCarthy, M.J., Dhir, R.K., 2005. Development of High Volume Fly Ash Cements for Use in Concrete Construction. *Fuel* 84, 1423-1432.

Mehta, P.K., 2009. Global Concrete Industry Sustainability. *Concrete International* 31, 45-48.

Mehta, P.K., 2004. High-Performance High-Volume Fly Ash Concrete for Sustainable Development. In *Proceedings of the International Workshop on Sustainable Development and Concrete Technology*, Beijing, China, p. 3-14.

Tatro, S.B., 2006. Thermal Properties. Chapter 22 in *ASTM STP 169D – Significance of Tests and Properties of Concrete & Concrete-Making Materials*. Eds. J.F. Lamond and J.H. Pielert, ASTM International, West Conshohocken, PA, p. 226-37.

Waller, V., De Larrard, F., Roussel, P., 1996. Modelling the Temperature Rise in Massive HPC Structures. in *4th International Symposium on Utilization of High-Strength/High-Performance Concrete*, RILEM, Paris, France, p. 415-421.

Zarr, R., 2000. NIST Standard Reference Database 81 - NIST Heat Transmission Properties of Insulating and Building Materials. Available at: <http://srdata.nist.gov/insulation/>, access verified October 2009.

Tables

Table 1. Mixture proportions for concretes A, B and C.

Concrete	FA, %	W/(C+FA)	Water, kg/m ³	Cement, kg/m ³	FA, kg/m ³	SSD Aggregates, kg/m ³		SP* L/m ³	28-d strength (MPa)
						Coarse	Fine		
A	0	0.50	211	425	----	734	990	2.2	43.5
	15			361	64	728	972		36.8
	30			298	128	741	963		32.5
	45			234	191	752	934		23.8
	60			170	255	743	923		16.8
	75			106	319	735	914		7.0
B	0	0.55	222	405	----	774	959	1.3	37.0
	15			344	61	772	941		32.4
	30			284	122	771	940		25.4
	45			223	182	770	904		19.6
	60			162	243	767	884		13.1
	75			101	304	770	904		6.0
C	0	0.60	222	370	----	785	973	0.6	32.1
	15			315	56	785	928		27.5
	30			259	111	787	921		21.3
	45			204	167	793	917		13.4
	60			148	222	785	883		9.8
	75			93	278	794	886		5.0

FA = Fly ash, C = Cement, SSD = Saturated surface dry

* Superplasticizer

Table 2. Measured heat capacities of powder materials for mortars.

Material	Density (kg/m ³)	Heat capacity [J/(g·K)]	Coefficient of Variation (%)
Type I/II cement	3250	0.74	0.69
Type III cement	3250	0.73	0.29
Class C fly ash	2690	0.73	0.12
Class F fly ash	2100	0.72	0.42
Gypsum	2320	1.02	1.15
Siliceous sand	2610	0.71	0.50
Lightweight sand	Not determined	0.65	0.02

Table 3. Measured heat capacities of powder materials for concretes.

Material	Density (kg/m ³)	Heat capacity [J/(g·K)]	Coefficient of Variation (%)
Type IP cement	3130	0.76	0.57
Class F fly ash	2380	0.72	0.31
Limestone sand	2650	0.76	0.20

Figures

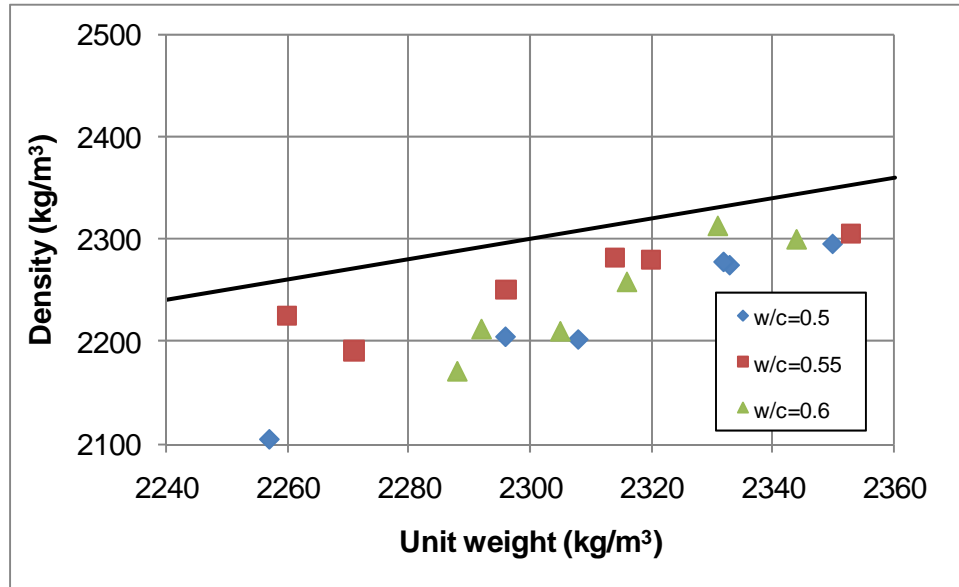


Figure 1. Densities measured on concrete cubes prior to cutting for thermal measurements vs. unit weights measured on fresh concretes in Mexico.

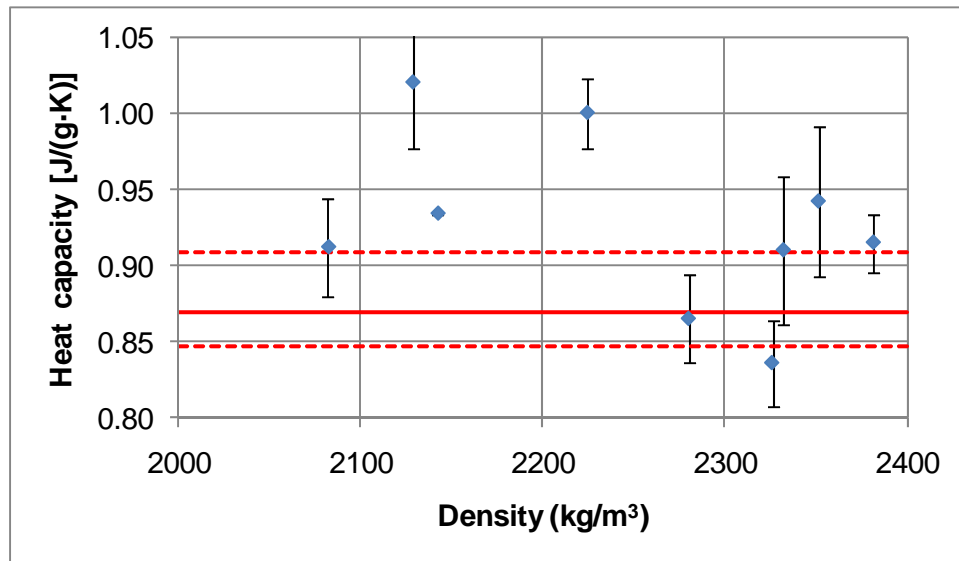


Figure 2. Heat capacities of HVFA mortars as a function of density. Solid line indicates average value of the bound water-based estimates while dashed lines indicate minimum and maximum values of the bound water-based estimates.

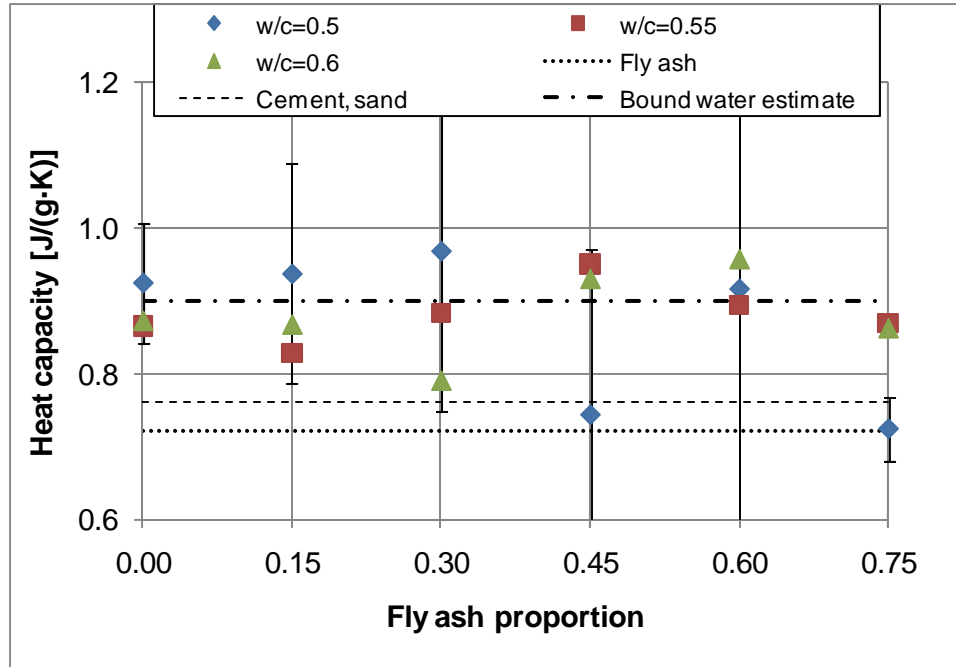


Figure 3. Heat capacities of HVFA concretes as a function of fly ash proportion (by mass). Dotted and dashed lines indicate measured values for fly ash and cement/sand, respectively. Dotted-dashed line indicates average value of bound water-based estimates. Standard deviations for $w/c=0.5$ mixtures are indicated by error bars.

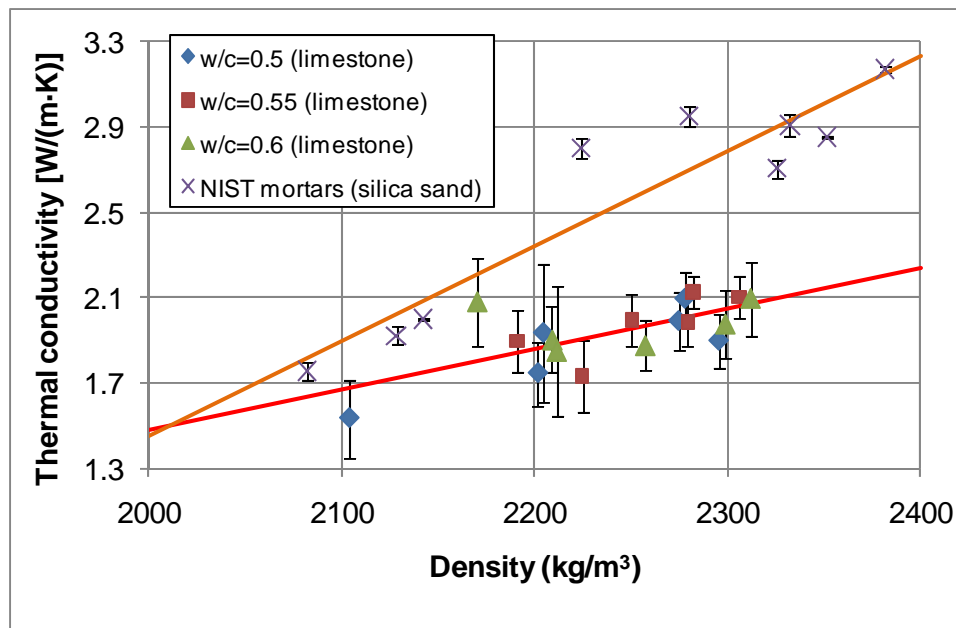


Figure 4. Measured thermal conductivities (with standard deviations indicated by error bars) for HVFA mortars and concretes examined in the study vs. measured density. Solid lines correspond to a linear fit for the concrete data given by $k = 0.0019 \cdot \rho - 2.32$ ($r=0.691$), and a linear fit for the mortars given by $k = 0.00445 \cdot \rho - 7.44$ ($r=0.935$).

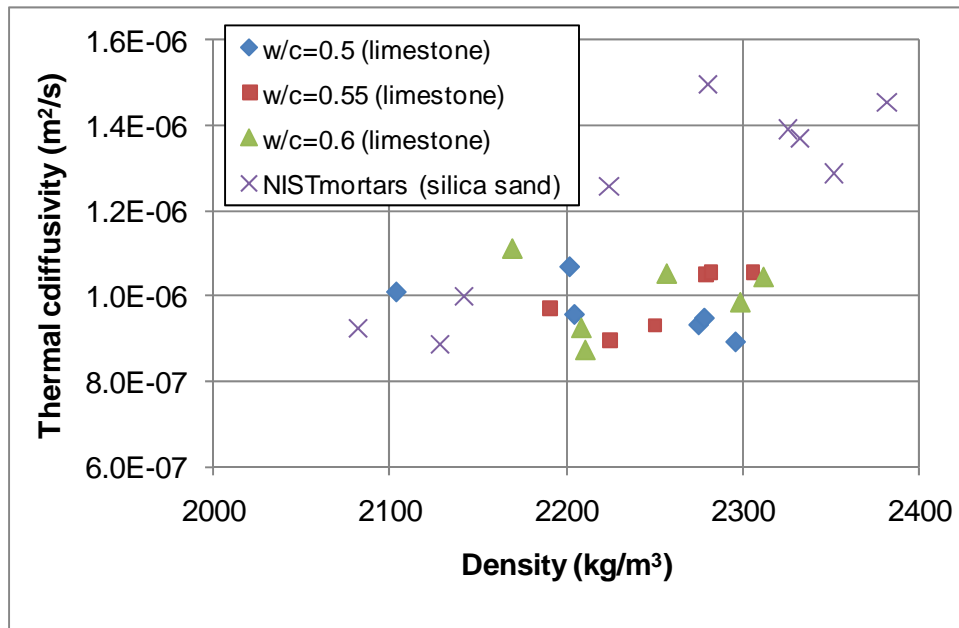


Figure 5. Computed thermal diffusivities for HVFA mortars and concretes examined in the study vs. measured density.